Available online at www.sciencedirect.com
ScienceDirect
Scripta Materialia 61 (2009) 327–330
Scripta MATERIALIA
www.elsevier.com/locate/scriptamat

Atomistic considerations of stressed epitaxial growth from the solid phase

N.G. Rudawski* and K.S. Jones

Department of Materials Science and Engineering, University of Florida, Gainesville, FL 32611-6400, USA

Received 11 March 2009; revised 8 April 2009; accepted 9 April 2009
Available online 14 April 2009

A dual-timescale model of stressed solid-phase epitaxial growth is developed to provide a basis for the atomistic interpretation of experiments where the macroscopic growth velocity of (0 0 1) Si was studied as a function of uniaxial stress applied in the plane of the growth interface. The model builds upon prior empirical modeling, but is a significant improvement as it provides solid physical bases as to the origin of growth being dual-timescale and more accurately models growth kinetics.

Keywords: Crystal growth; Phase transformations; Phase transformation kinetics; Kinetics; Solid-phase epitaxial growth

The epitaxial amorphous (α) to crystalline phase transformation under applied mechanical stress, or stressed solid-phase epitaxial growth (SPEG), has been a topic of fundamental [1–14] and technological [15–19] interest for many years. However, although the macroscopic considerations of the stressed-SPEG process have been studied in several different materials systems under many different states of applied stress, the atomistic considerations of the process are somewhat poorly understood.

Prior work [3] modeled the velocity of the α/crystalline (growth) interface, v, with an applied stress state, σ_{ij}, as a generalization of the continuous growth model of Wilson [20] (which does not address atomic-level processes and is single timescale) based on the strong Arrhenius-type [21] behavior [22,23] of v. This approach explained pure hydrostatic [1,2] and normal uniaxial compression-enhanced growth [6] (albeit with some inconsistency [12]), but could not be reasonably extended to explain cases of growth where uniaxial [10–14] or biaxial stress [7] was applied in the plane of the growth interface.

After observing compelling, highly-repeatable data for v in (0 0 1) Si as a function of σ_{11} applied along [1 1 0] (uniaxial stress in the plane of the growth interface), where v with $\sigma_{11} > 0$ (tension) was unchanged from the stress-free case and v with $\sigma_{11} < 0$ (compression) was retarded to an asymptotic value, Rudawski et al. [12] advanced the possibility of SPEG being a multiple-timescale process. Specifically, v in (0 0 1) Si as a function of σ_{11} was empirically modeled as

$$v = \frac{h}{\tau_A(0) + \tau_B(0)\exp\left(\frac{-\Delta V_{11}^B \sigma_{11}}{kT}\right)} + \frac{h}{\tau_A(0) + \tau_B(0)} \qquad (1)$$

where $\tau_A(0)$ and $\tau_B(0)$ are the $\sigma_{ij} = 0$ values of two arbitrary timescales associated with atomic-level growth processes, $h = 0.14$ nm is the monolayer height, kT has the usual meaning and ΔV_{11}^B is the activation volume associated with τ_B when σ_{11} is applied. For SPEG at $T \leqslant 525$°C, this empirical approach was able to qualitatively and quantitatively explain the observed v vs. σ_{11} behavior [11–14], but could not quantitatively account for growth at $T \geqslant 550$ °C. Additionally, the atomistic origins of τ_A and τ_B were unclear.

In this letter, a dual-timescale modeling approach to explain the compelling experimental results from Rudawski et al. [12] is presented. However, rather than employing an empirical approach, the origins of each timescale, one associated with island nucleation and the other with island ledge migration, are rigorously derived from atomistic considerations of growth from the solid phase, thus providing a clear theoretical framework to understanding the role of applied stress on SPEG. Additionally, the model is shown to be capable of greater quantitative agreement with observed stressed-SPEG data (compared to the prior empirical [12] model) for a range of growth temperatures and therefore provides a significant improvement in the

* Corresponding author. E-mail: ngr@ufl.edu

1359-6462/$ - see front matter © 2009 Acta Materialia Inc. Published by Elsevier Ltd. All rights reserved.
doi:10.1016/j.scriptamat.2009.04.015

understanding of the atomistic nature of the stressed-SPEG process.

SPEG has been likened to liquid-phase epitaxial growth, of which the atomistics have been addressed for some time [20,24,25]. Defining a coordinate frame of reference, the one and two axes lie within the growth interface, with axis three parallel to the macroscopic growth direction. When growth is thermodynamically favorable on an atomically sharp growth interface, initial crystal island nuclei with height h form on the interface and the island ledges propagate laterally within the plane of the growth interface with velocities $v_{m,1}$ and $v_{m,2}$. When the island reaches a minimum area, $A_{\min}$, a second island will nucleate on top of the first one. This process is shown schematically in Figure 1. The timescale, τ, for this process to complete (assuming an effectively infinite growth interface) relates to the macroscopic growth velocity via

$$v = \frac{h}{\tau} = h\left(\frac{\pi v_{m,1} v_{m,2}}{A_{\min}}\right)^{1/2} \tag{2}$$

which can be equivalently written in terms of the rate of nucleation per unit area, J [24]. This model assumes that ledges may propagate from a nucleus with initial radius, r_0, essentially zero. However, a cylindrical island with <1 1 0>-aligned ledges (believed to be the case for any α-Si/Si interface not atomically sharp [26]) must achieve radius

$$r^* = \frac{-\gamma_L}{\Delta G_v h} \sim \frac{-\gamma_{\{011\}}}{\Delta G_v} \tag{3}$$

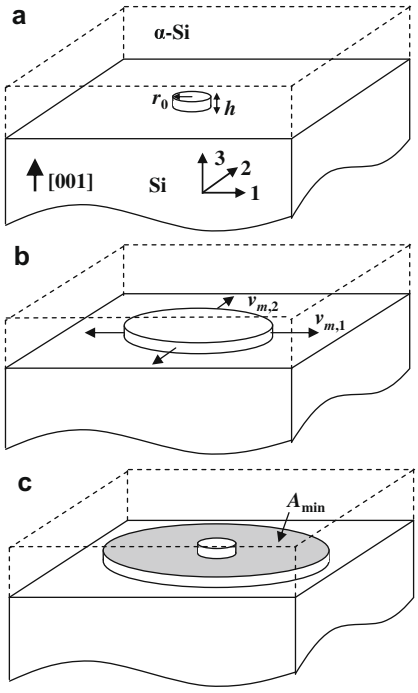

Figure 1. Atomistic schematics of the SPEG process: (a) nucleation of an initial island with radius r_0 and monolayer height h, followed by (b) in-plane migration of island ledges with velocities $v_{m,1}$ and $v_{m,2}$, followed by (c) the island achieving area $A_{\min}$ such that the nucleation of a second island with r_0 can occur on top of the original island. The monolayer height divided by the total time elapsed between (a) and (c) corresponds to the macroscopic growth velocity.

before being stable, where γ_L is the step-edge tension (approximately equal to the α-Si/{0 1 1} Si interfacial energy, $\gamma_{\{011\}}$, multiplied by h) and ΔG_v is the free energy difference per unit volume. Thus, after an underlying island achieves $A_{\min}$, only through random atomic vibrations can a new island with $r_0 = r^*$ form, which requires a finite amount of time. This timescale, referred to as the nucleation timescale, τ_n, is instantaneous for $r_0 = 0$, but is non-negligible if $r_0 \neq 0$.

Thus, the growth process is separated into two timescales: τ_n and the migration timescale, τ_m, which is the time required for an island to achieve $A_{\min}$ after initial nucleation via migration of the island ledges with

$$v = \frac{h}{\tau_n + \tau_m} \tag{4}$$

Determining τ_n first requires determining the number of crystalline bonds, N, which must form to nucleate an island with $r_0 = r^*$. For the case of (0 0 1) SPEG, this is given by $N = \pi r^{*2} h \rho_v n_v/2$, where $\rho_v = 5 \times 10^{22}$ cm^{-3} and $n_v = 4$ are the atomic density and coordination number as shown in Figure 2. Using the reported heat of crystallization $\Delta H_c = 12$ kJ mol^{-1} [27] and the calculated planar {0 1 1} atomic density $\rho_{\{011\}} = 9.7 \times 10^{18}$ m^{-2}, $\gamma_{\{011\}} = 0.85 \Delta H_c \rho_{\{011\}} = 0.2$ J m^{-2} (from Spaepen [28]) with $\Delta G_v \sim 6.7 \times 10^8$ J m^{-3} [27]. Thus, $r^* \sim 0.22$ nm (reasonably independent of temperature). It is then calculated that, for the case of (0 0 1) Si ($h = 0.14$ nm), $N \sim 4$ bonds must be rearranged.

In relating τ_n to N, consider that (i) SPEG typically occurs far from equilibrium [23] and (ii) the α-Si phase is essentially a distortion [28] of bond lengths and angles of the crystalline counterpart, and correcting these distortions is accomplished by breaking and reforming bonds. The probability of the bond of an atom in the neighboring amorphous phase fluctuating and resulting in being the correct position to form crystalline material is given by

$$P = \frac{1}{Z(E)} \exp\left(\frac{-E_n}{kT}\right) \tag{5}$$

where E_n is the energy of the activated transition state (close to the energy required to break a Si–Si bond) and $Z(E)$ is the partition function. Thus,

$$\frac{1}{\tau_n} = \frac{P\omega}{n_v N} \tag{6}$$

where ω is the atomic vibration frequency.

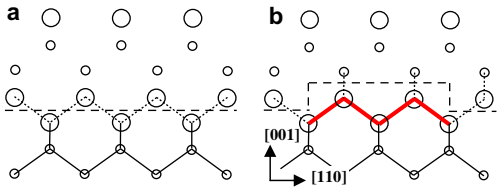

Figure 2. Atomistic schematics of island nucleation on an α-Si/(0 0 1) Si interface: (a) an initially planar interface and (b) after nucleation of an island. The thick black dashed line, thin black dashed lines, thin black solid lines and thick red solid lines represent the α/crystalline interface, bonds across the interface, bonds within pre-existing crystalline material and crystalline bonds formed within the nucleated island, respectively. (For interpretation of the references to color in this figure legend, the reader is referred to the web version of this paper.)

Once a nuclei with $r_0 = r^*$ has formed, ledge migration can commence. The relationship between τ_m, $A_{\min}$, r_0, $v_{m,1}$ and $v_{m,2}$ is easily shown to be parabolic in nature as given by

$$\tau_m = \frac{-\pi r^*(v_{m,1}+v_{m,2}) + \sqrt{\pi^2 r^{*2}(v_{m,1}+v_{m,2})^2 - 4\pi v_{m,1}v_{m,2}(\pi r^{*2} - A_{\min})}}{2\pi v_{m,1}v_{m,2}} \tag{7}$$

Since SPEG typically occurs far from equilibrium [25] and ledge motion does not require the generation of excess interfacial area, the ledge velocity along the ith in-plane direction can be defined as $v_{m,i} = M_{ij}\Delta x_j$, where M_{ij} is the ledge mobility tensor and Δx_j is the ledge migration vector with M_{ij} isotropic for (0 0 1)-oriented growth. Since ledge mobility is related to the rate at which bonds in the adjacent amorphous phase can rearrange and form crystalline material, similarly to the case of nucleation, M_{ij} can be further defined as $M_{ij} = M_{ij0}\exp(-E_{m,ij}/kT)$, where $E_{m,ij}$ and M_{ij0} are the activation energy and pre-exponential factor for component ij.

Next, the role of applied stress on each timescale can be determined by understanding the volumetric deformation associated with the transition state of each process. For the case of τ_n (a scalar), the effect of applied stress is given by

$$\frac{1}{\tau_n} = \frac{1}{\tau_n(0)}\exp\left(\frac{\Delta V^n_{ij}\sigma_{ij}}{kT}\right) \tag{8}$$

where $\tau_n(0)$ is the stress-free value of τ_n and ΔV^n_{ij} is the activation volume tensor associated with the nucleation transition state (assuming negligible change to ω from σ_{ij}). Forming an island causes deformation primarily along the growth direction (analogous to interstitial formation near a surface [29]) and, thus, considering necessary symmetry constraints, only ΔV^n_{33} is non-zero in ΔV^n_{ij} for the α-Si/(0 0 1) Si interface. Therefore, only σ_{33} can alter τ_n.

The case of ledge migration is different from nucleation since $v_{m,i}$ is proportional to mobility, a second-order tensor, with

$$M_{ij} = M_{ij}(0)\exp\left(\frac{\Delta V^{m,ij}_{kl}\sigma_{ij}}{kT}\right) \tag{9}$$

where $M_{ij}(0)$ is the stress-free version of M_{ij} and $\Delta V^{m,ij}_{kl}$ is the activation volume tensor associated with ledge mobility (a fourth-order tensor). In the case of a ledge migrating within the growth interface, the associated transition state will predominantly have a volumetric deformation component aligned with a given migration direction (longitudinal), $\Delta V^{m,11}_{11}$ for $v_{m,1}$ (equivalent to $\Delta V^{m,22}_{22}$ for $v_{m,2}$), and the macroscopic growth direction (transverse), $\Delta V^{m,11}_{33}$ for $v_{m,1}$ (equivalent to $\Delta V^{m,22}_{33}$ for $v_{m,2}$). Thus, if σ_{11} is applied, $v_{m,1}$ will be influenced as given by $v_{m,1} = M_{11}(0)\Delta x_1\exp(\Delta V^{m,11}_{11}\sigma_{11}/kT)$ while $v_{m,2}$ will be unchanged; application of σ_{33} would alter $v_{m,1}$ and $v_{m,2}$ equally. Combining and manipulating the necessary equations, v as a function of σ_{11} is given by

$$v = \frac{h}{\tau_n(0) + \frac{1}{v_{m,1}(0)}\left(\frac{A_{\min}}{\pi r^*} - r^*\right)\left[1 + \frac{2\pi(A_{\min}-\pi r^{*2})}{r^*\left(\sqrt{\pi A_{\min}}-\pi r^*\right)}\exp\left(\frac{\Delta V^{m,11}_{11}\sigma_{11}}{kT}\right)\right]^{-1}} \tag{10}$$

where $v_{m,1}(0) = M_{11}(0)\Delta x_1$. Eq. (10) was fitted to the observed (0 0 1)-oriented v vs. σ_{11} (along the in-plane [1 1 0] direction) data from Rudawski et al. [12] for different T using least-squares regression analysis, as shown in Figure 3, with the predicted behavior of Eq. (1), the prior empirical dual-timescale model [11,12], provided for reference. For each T, $\sigma_{11} > 0$ did not appreciably change v compared to the stress-free case, while $\sigma_{11} < 0$ tended to retard v to a limiting value. For $T \leqslant 525$ °C, Eq. (1) matches well with the observed v vs. σ_{11} behavior, but has significant negative deviation for $\sigma_{11} < 0$ when $T \geqslant 550$ °C. However, Eq. (10) provides excellent agreement with the observed v vs. σ_{11} behavior for all T. The values of $\tau_n(0)$, $v_{m,1}(0)$, $A_{\min}$, and $\Delta V^{m,11}_{11}$ obtained by fitting Eq. (10) to the data from Rudawski et al. [12] for each value of T are shown in Table 1, with $\tau_n(0)$ and $v_{m,1}(0)$ decreasing and increasing with increasing temperature, respectively. $A_{\min}$ and $\Delta V^{m,11}_{11}$ both appear to be temperature-independent, with typical values of ~50 nm^2 and ~12 Ω, where Ω is the atomic volume of Si. The behavior of the logarithm of $\tau_n(0)^{-1}$ and $v_{m,1}(0)$ vs. the reciprocal of kT is highly linear (not presented) and indicates that each process is Arrhenius in nature, as expected, with $E_n = 2.5 \pm 0.1$ eV (assuming T-independent ω, which is reasonable for the temperatures studied by Rudawski et al. [12]) and $E_{m,11} = 2.8 \pm 0.2$ eV extracted.

The apparent temperature-independence of $\Delta V^{m,11}_{11}$ is reasonable and expected since it is related to the volumetric deformation associated with each localized atomistic transition state and it was shown that $E_{m,11}$ is constant over this temperature range. The relatively large magnitude of $\Delta V^{m,11}_{11}$ (compared with most processes which occur in bulk Si [30]) is indicative of

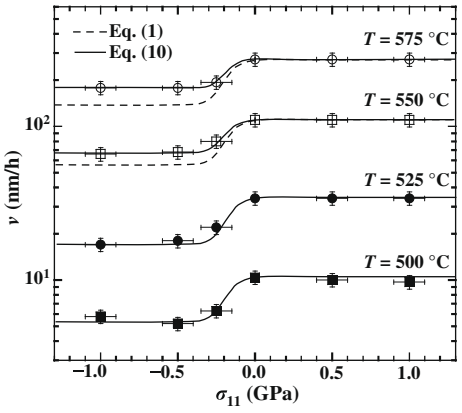

Figure 3. Plot of the measured (0 0 1)-oriented growth velocity (v) vs. applied in-plane uniaxial stress along [1 1 0] (σ_{11}) for annealing temperatures T of 500–575 °C from Rudawski et al. [12]. The v vs. σ_{11} behavior fits using Eq. (1) (prior empirical dual-timescale model [12]) and Eq. (10) (new dual-timescale model) are provided for reference. For $T \leqslant 525$ °C, Eqs. (1) and (10) provide essentially indistinguishable fits.

Table 1. The T-dependence of $\tau_n(0)$, $v_{m,1}(0)$, $A_{\min}$ and $\Delta V_{11}^{m,11}$ as determined by fitting Eq. (10) to the data of Figure 3.

T (°C)	$\tau_n(0)$ (s)	$v_{m,1}(0)$ (nm s^{-1})	$A_{\min}$ (nm^2)	$\Delta V_{11}^{m,11}$ (Ω)
500	48.6 ± 5.0	2.4 ± 0.1	49 ± 5	13 ± 1
525	14.8 ± 2.0	8.0 ± 0.8	52 ± 5	12 ± 1
550	4.5 ± 0.5	38.0 ± 4.0	51 ± 5	12 ± 1
575	1.8 ± 0.2	96.0 ± 9.0	42 ± 4	14 ± 1

coordinated atomic motion during ledge migration, which has been analogously described elsewhere [11,31].

Regarding the apparent temperature-independence of $A_{\min}$, it can be shown that [24,32]

$$A_{\min} = \left(\frac{3\pi v_{m,1} v_{m,2}}{J^2}\right)^{1/3} \tag{11}$$

(assuming $r_0 = 0$), therefore implying ledge mobility has the same temperature-dependence as J. This is intuitive and reasonable, since both ledge migration and island nucleation are controlled by the same process of bond breaking and rearrangement; with the system typically far from equilibrium during SPEG [25], kinetic limitations effectively control growth. This is supported by the observation that $E_n \approx E_{m,11}$.

As a final note, though it is not shown here, it is possible to generalize v with any arbitrary σ_{ij} using the model presented to explain prior results of stressed-SPEG where different stress states were applied [1–14].

In summary, a dual-timescale model of stressed SPEG was presented to explain the compelling stress-dependent growth kinetics observed in prior work. This approach builds upon prior speculations and empirical modeling of growth being dual-timescale, but is a significant improvement in that the newly developed framework has solid atomistic bases (as per related work in growth from the liquid phase) and can more accurately model stressed growth kinetics.

The authors acknowledge S.R. Phillpot from the University of Florida for thoughtful discussions.

[1] E. Nygren, M.J. Aziz, D. Turnbull, J.M. Poate, D.C. Jacobsen, R. Hull, Appl. Phys. Lett. 47 (1985) 232.
[2] G.Q. Lu, E. Nygren, M.J. Aziz, J. Appl. Phys. 70 (1991) 5323.
[3] M.J. Aziz, P.C. Sabin, G.Q. Lu, Phys. Rev. B 44 (1991) 9812.
[4] Q.-Z. Hong, J.G. Zhu, J.W. Mayer, W. Xia, S.S. Lau, J. Appl. Phys. 71 (1992) 1768.
[5] C. Lee, T.E. Haynes, K.S. Jones, Appl. Phys. Lett. 62 (1993) 501.
[6] W. Barvosa-Carter, Ph.D. Thesis, Harvard University, 1997.
[7] M.S. Phen, R.T. Crosby, V. Craciun, K.S. Jones, M.E. Law, J.L. Hansen, A.N. Larsen, Mater. Res. Soc. Symp. Proc. 864 (2005) E4.28.1.
[8] W. Barvosa-Carter, M.J. Aziz, L.J. Gray, T. Kaplan, Phys. Rev. Lett. 81 (1998) 1445.
[9] J.F. Sage, W. Barvosa-Carter, M.J. Aziz, Appl. Phys. Lett. 77 (2000) 516.
[10] N.G. Rudawski, K.S. Jones, R. Gwilliam, Appl. Phys. Lett. 91 (2007) 172103.
[11] N.G. Rudawski, K.S. Jones, R. Gwilliam, Phys. Rev. Lett. 100 (2008) 165501.
[12] N.G. Rudawski, K.S. Jones, R. Gwilliam, Mater. Sci. Eng. R. Rep. 61 (2008) 40.
[13] N.G. Rudawski, K.S. Jones, R. Gwilliam, Appl. Phys. Lett. 92 (2008) 232110.
[14] N.G. Rudawski, K.S. Jones, R. Gwilliam, J. Mater. Res. 24 (2009) 305.
[15] Y.G. Shin, J.Y. Lee, M.H. Park, H.K. Kang, Jpn. J. Appl. Phys. 40 (2001) 6192.
[16] C.R. Olson, E. Kuryliw, B.E. Jones, K.S. Jones, J. Vac. Sci. Technol. B 24 (2006) 446.
[17] N.G. Rudawski, K.N. Siebein, K.S. Jones, Appl. Phys. Lett. 89 (2006) 082107.
[18] N.G. Rudawski, K.S. Jones, R.G. Elliman, J. Vac. Sci. Technol. B 26 (2008) 435.
[19] N.G. Rudawski, K.S. Jones, S. Morarka, M.E. Law, R.G. Elliman, J. Appl. Phys. 105, (2009) 081101.
[20] H.A. Wilson, Philos. Mag. 50 (1900) 238.
[21] A.N. Kolmogorov, Izv. Akad. Nauk SSSR Ser. Math. 3 (1937) 355.
[22] S.D. Peteves, R. Abbaschian, Metall. Trans. A 22A (1991) 1271.
[23] S. Glasstone, K.J. Laidler, H. Eyring, The Theory of Rate Processes, McGraw-Hill, New York, 1948.
[24] G.A. Olson, J.A. Roth, Mater. Sci. Rep. 3 (1988) 1.
[25] J.A. Roth, G.L. Olson, D.C. Jacobson, J.M. Poate, Appl. Phys. Lett. 57 (1990) 1340.
[26] J.S. Williams, R.G. Elliman, Phys. Rev. Lett. 51 (1983) 1069.
[27] E.P. Donovan, F. Spaepen, D. Turnbull, J.M. Poate, D.C. Jacobson, Appl. Phys. Lett. 42 (1983) 698.
[28] F. Spaepen, Acta Metall. 26 (1978) 1167.
[29] M.J. Aziz, Appl. Phys. Lett. 70 (1997) 2810.
[30] P.M. Fahey, P.B. Griffin, J.D. Plummer, Rev. Mod. Phys. 61 (1989) 289.
[31] R.J. Asaro, S. Suresh, Acta Mater. 53 (2005) 3369.
[32] M. Volmer, M. Marder, Z. Phys. Chem. A154 (1931) 97.